International Compressor Engineering Conference

School of Mechanical Engineering

2021

Investigation of Back-Diffusion Losses in an Electrochemical Hydrogen Compressor

Ashish Chouhan
University of Delaware

Bamdad Bahar
Xergy Inc., Bamdad.bahar@xergyinc.com

Ajay K. Prasad
University of Delaware

Investigation of Back-Diffusion Losses in an Electrochemical Hydrogen Compressor

Ashish CHOUHAN[1], Bamdad BAHAR[2*], and Ajay K. PRASAD[1]

[1]Department of Mechanical Engineering, University of Delaware, Newark, DE 19716

[2]Xergy Inc., Harrington, DE 19952 (bamdad.bahar@xergyinc.com, Tel: 302 218 4279)

ABSTRACT

Hydrogen offers the potential to decarbonize the automotive and stationary power sectors and is therefore expected to play an increasingly significant role in meeting global energy demand. However, due to its low volumetric and gravimetric energy densities, it is important to find methods to efficiently store hydrogen in order to grow the hydrogen economy. Storing hydrogen as a compressed gas could be achieved by electrochemical compression (ECC), which is a membrane-based alternative to conventional mechanical compressors. ECC can be superior to mechanical compressors because of its higher efficiency, lack of moving parts and noiseless operation. Here, we report on the ECC of hydrogen using a Nafion 115 membrane at room temperature. Pressure vs. time curves have been collected at various operating voltages, and a compression ratio of 150 has been achieved with a single cell at an operating voltage of 0.1 V. This work focuses on analyzing the contribution of back-diffusion to the performance of an electrochemical hydrogen compressor.

1. INTRODUCTION

Greenhouse gas emissions from the combustion of fossil fuels in responsible for climate change. With a rapid increasing in the world energy demand, it is imperative to develop energy generation and conversion technologies that are not based on fossil fuels. One viable clean-energy alternative is hydrogen which can be produced renewably in a carbon-free manner and used to generate electricity with environmentally friendly and energy-efficient devices like fuel cells. Hydrogen is therefore an attractive fuel for both stationary and automotive applications. However, being the lightest gas, hydrogen is difficult to store either as a compressed gas or as a liquid. According to the DOE [1], the ultimate targets for gravimetric and volumetric efficiency of hydrogen storage are 2.2 kWh/kg and 1.7 kWh/L, respectively. In comparison, the state-of-the-art efficiencies are 1.4 kWh/kg and 0.8 kWh/kg. Creating and expanding the hydrogen economy of the future requires advances in the field of hydrogen storage.

Storing hydrogen as a compressed gas is often preferred because of the simplicity of the process. Hydrogen is typically compressed using a mechanical compressor which has moving parts and requires frequent maintenance, adding to cost and complexity. One alternative to mechanical compression is electrochemical compression (ECC). Electrochemical compression is superior to mechanical compression because it ensures noiseless operation due to a lack of moving parts. Moreover, for lower power applications, ECC is more efficient than mechanical compression and is less prone to failure. ECC is also attractive for refrigeration and air-conditioning systems because it can replace conventional mechanical compressors while permitting the use of environmentally friendly refrigerant gases.

These multi-fold advantages over mechanical compression make ECC an attractive candidate for pressurization applications. In this paper, we will focus on ECC of hydrogen.

ECC of hydrogen (i.e. hydrogen pumping) based on polymer electrolyte membranes (PEM) was originally developed several decades ago [2, 3]. ECC is accomplished with an electrochemical cell, whose assembly is shown schematically in Figure 1. The ECC consists of a membrane electrode assembly (MEA) and gaskets, two bipolar plates with gas flow channels, and two end plates for cell compression. When an external voltage is applied across the electrodes, hydrogen entering the ECC at the anode undergoes oxidation to generate protons and electrons. The protons migrate through the PEM to the cathode, while the electrons pass through an external circuit and recombine with the protons at the cathode to produce hydrogen at an elevated pressure [4, 5, 6]. The anode and cathode reactions are shown below:

$$H_2 \text{ (low P)} \rightarrow 2H^+ + 2e^- \qquad \text{(Anode)} \qquad (1)$$

$$2H^+ + 2e^- \rightarrow H_2 \text{ (high P)} \qquad \text{(Cathode)} \qquad (2)$$

The overall electrochemical reaction can be written as:

$$H_2 \text{ (anode, low pressure)} \rightarrow H_2 \text{ (cathode, high pressure)} \qquad (3)$$
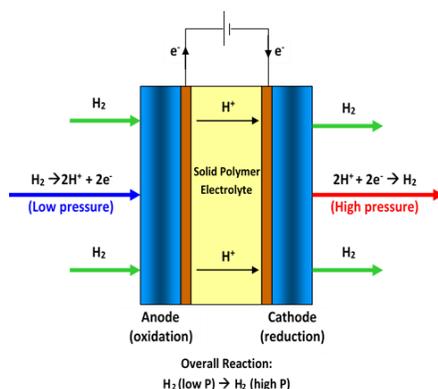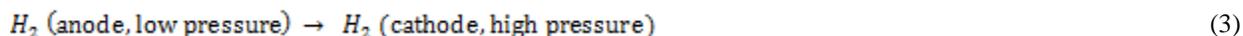

Figure 1. Schematic of an electrochemical cell for the compression of hydrogen.

Figure 1 reveals that the hardware for ECC is identical to PEM fuel cells. While PEM fuel cells have been investigated extensively over the past decades, the literature for ECC is rather sparse. Rohland et al. [4] used Nafion membranes to conduct ECC experiments at STP and showed a somewhat linear behavior between voltage and current density. Strobel et al. [5] demonstrated the ability to reach high cathode pressures and evaluated the back-diffusion rate and diffusion coefficients for different membranes tested. Sedlak et al. [7] demonstrated the use of PEM for electrochemically pumping and purifying hydrogen. Wong et al. [8] used a stack assembly of multiple cells connected in series to achieve high pressures up to 85 MPa. Similarly, Bouwman et al. [9, 10] used a series configuration to compress hydrogen to pressures as high as 100 MPa. More recently, Nordio et al. [11] undertook experimental and modeling studies to investigate the electrochemical separation and compression of hydrogen from nitrogen and methane. Suermann et al. [12] studied electrochemical losses related to gas crossover due to hydrogen pressurization up to 5 MPa. Grigoriev et al. [13] employed PEM to pressurize hydrogen to 5 MPa in a single step using a small voltage of 0.140 V. Nguyen et al. [14] investigated the performance of an electrochemical hydrogen

compressor at different operating conditions and pointed out its limits at low inlet hydrogen concentrations. Perry et al. [15] used a high temperature polybenzimidazole membrane for electrochemical hydrogen pumping and tested its durability under typical operating conditions for 4000 hrs. Kee et al. [16] used a thermodynamics-based approach to compare the performance of electrochemical hydrogen compressors at low temperature using a polymer-based PEM (e.g. Nafion) and at high temperature using a ceramic-based PEM (e.g. yttrium-doped barium zirconates).

Perfluorosulfonic acid (PFSA) membranes like Nafion have been extensively used for both fuel cell and ECC applications because of their superior mechanical and chemical durability and high proton conductivity. However, Nafion also permits the back-diffusion of molecular hydrogen which can limit the maximum achievable pressure. Most of the previous studies focused on achieving higher pressures. In this paper, we focus on the effect of back diffusion and develop a theoretical basis for the effect of back diffusion on the cathode pressure and the overall performance of the ECC.

2. EXPERIMENTAL PROCEDURE

The experiments were carried out using a single cell apparatus with an active area of 25 cm^2 provided by Xergy, Inc. The end plates (2.5 cm thick) and bipolar plates (0.6 cm thick) with parallel flow field channels were machined out of aluminum. Each flow field channel was 50 mm long, 2 mm wide and 2 mm deep, and adjoining channels were separated by a 2.5 mm wide rib. Nafion 115 (thickness 125 µm) was used as the membrane, and the electrodes used to fabricate the membrane electrode assemblies (MEA) had a platinum (Pt) catalyst loading of 0.3 mg/cm^2 on Vulcan-carbon cloth, purchased from Fuel Cell Store. Mylar gaskets were used between the MEA and the flow fields to ensure a good seal. The MEAs were prepared by hot-pressing under a load of 0.5 metric tons at 80°C for 2 minutes. All of the electrochemical compression tests reported here were carried out using an Arbin Fuel Cell Test Stand.

The ECC experiments reported here were conducted at room temperature (22°C). Nafion only conducts protons when properly hydrated. Therefore, the inlet hydrogen stream to the anode was fully humidified. The anode flow rate was set to 100 cm^3/min, which was sufficiently high to preclude mass transport losses even at the highest currents. The anode outlet was open to the atmosphere and so the anode pressure was maintained at 1 atm. The cathode port was closed off with a pressure transducer (OMEGA PX309-10KG5V). A stainless-steel mesh was placed between the MEA and the bipolar plates to provide structural support to the MEA and ensure that it was not deformed under the very high differential pressures developed during the experiments, thereby mitigating the possibility of MEA failure. To ensure proper sealing at high pressures, O-rings were installed in the bipolar plates. The end plates were held together with eight bolts, each tightened to a torque of 90 N-m. Experiments were performed at four operating voltages: 0.025, 0.05, 0.075, and 0.1 V. Each experiment was continued until the current and pressure reached equilibrium.

3. RESULTS AND DISCUSSION

The rate of hydrogen production at the cathode or forward flux $(\dot{n}_f)$ is directly related to the current drawn by the compressor according to Faraday's law [17]:

$$\dot{n}_f = \frac{I}{zF} \tag{4}$$

where $\dot{n}_f$ is the mol/s of hydrogen generated, I is the current in amperes, $F = 96485 \text{ C/mol}$ is Faraday's constant, and z is the number of electrons per molecule of hydrogen. As shown by Equations 1 and 2, $z = 2$ for the ECC of hydrogen. The Nernst equation specifies the ideal voltage required to attain the desired compression ratio:

$$E_{Nernst} = E_o + \frac{RT}{2F} \ln\left(\frac{P_c}{P_a}\right) \tag{5}$$

where R is the universal gas constant ($8.314 \text{ Jmol}^{-1}\text{K}^{-1}$), T is the operating temperature in K, P_c is the cathode pressure, and P_a is the anode pressure. E_o is the standard electrode potential and is equal to zero as the half-cell reactions at the anode and cathode are the same.

The variation of pressure and current density with time during the compression process is presented in Figure 2 for all four voltages. For each applied voltage, the cathode pressure (blue curve) rises rapidly at the start of the operation and eventually plateaus to an equilibrium value. Concurrently, the current density (red curve) is the highest at the start and declines rapidly at first before gradually reaching an equilibrium value after a few hours. As shown in Figure 3, the equilibrium compression ratio $(P_{c,eq}/P_a)$ increases with the applied voltage as predicted by Equation 5. Figure 3 also shows that the initial current density increases linearly with voltage. Likewise, the equilibrium current density also increases roughly linearly with voltage. The equilibrium current density is about an order of magnitude smaller than the initial value.

The fact that the equilibrium current density is non-zero although the cathode pressure has equilibrated indicates that back-diffusion is occurring. In fact, the equilibrium current when converted to a molar flux by Faraday's Law is an exact measure of the backward flux due to Fickian diffusion. The rate of back diffusion is proportional to the pressure differential across the membrane and therefore, at elevated pressures, a higher current is required to overcome the back-diffusive flux.
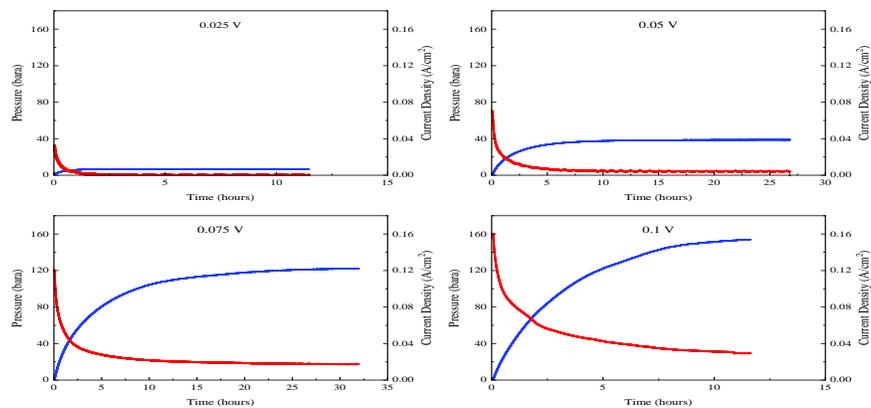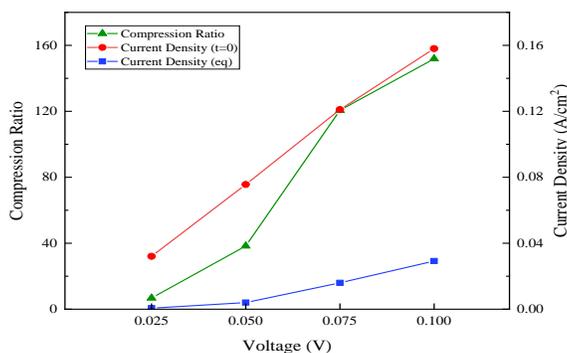
Figure 2. Pressure (blue) and current density (red) vs. time for Nafion 115 – 4 Voltages

Figure 3. Initial current density, equilibrium current density, and equilibrium compression ratio - 4 applied voltages.

According to Equation 5, the ideal cathode pressures corresponding to 0.025, 0.05, 0.075, and 0.1 V should be 7.24, 51.8, 370, and 2647 bara, respectively. In contrast, the corresponding steady-state pressures are measured as 6.84, 38.8, 122, and 154 bara. Clearly, the steady-state pressures shown in Figures 2 and 3 cannot match the predicted values. For a given compression ratio, the supplied voltage E_{cell} has to be larger than the Nernst voltage in order to overcome all the irreversibilities associated with ECC operation including activation overpotentials at the anode and cathode, ohmic resistance, mass transport losses, and back diffusion:

$$E_{cell} = E_{Nernst} + \Delta E_{Activation} + \Delta E_{Ohmic} + \Delta E_{Transport} + \Delta E_{Back\ Diffusion} \tag{6}$$

where $\Delta E_{Activation}$ is the sum of activation overpotentials η_a and η_c at the anode and cathode, respectively. ΔE_{Ohmic} is the sum of ohmic losses associated with the membrane resistance and contact resistances between the cell components, with membrane impedance being the dominant factor. At high current densities, mass transport losses denoted by $\Delta E_{Transport}$ could become significant due to the inability of the reactant gas to approach the anode catalytic sites fast enough. Mass transport losses could also arise because of water flooding the flow field channels and/or saturating the gas diffusion layers, low porosity of the electrodes or any other factor that restricts the reactant flow. $\Delta E_{Back\ Diffusion}$ represents losses due to back diffusion of hydrogen from the pressurized cathode to the anode through the membrane. All of these losses cause the required voltage to exceed the Nernst voltage for a given compression ratio.

In the ECC of hydrogen, $\Delta E_{Activation}$ is expected to be small because of the fast reaction kinetics of hydrogen oxidation and reduction. Since the compressor operates at fairly low voltages, the current generated is relatively small so reactant starvation is not expected to be significant, and thus $\Delta E_{Transport}$ is also small. ΔE_{Ohmic} could be reduced by employing thinner membranes, however, thinner membranes may not be able to withstand the high pressures being generated and could be more susceptible to failure. Thus, it is essential to find an optimal membrane thickness for the hydrogen compressor. The need to optimize membrane thickness becomes even more important when we consider back-diffusion. If we convert the measured steady-state pressures listed above at the applied voltages of 0.025, 0.05, 0.075 and 0.10 V to their corresponding Nernstian voltages using Equation 5, we would obtain values of 0.024, 0.046, 0.061, and 0.064 V, respectively. The difference between the applied and Nernstian voltage increases rapidly with the compression ratio and clearly indicates that back-diffusion is playing a

dominant role. As the pressure builds at the cathode with the anode still being at atmospheric pressure, the pressure differential forces hydrogen to permeate through the membrane back to the anode. This poses a barrier in achieving higher pressures. The backward diffusive flux is $(\dot{n}_b)$ as given by Fick's law is directly proportional to the difference in hydrogen concentration (ΔC) across the membrane and inversely proportional to the membrane thickness (d):

$$\dot{n}_b = -DA\frac{\Delta C}{d} \tag{7}$$

where D is the diffusivity of hydrogen in the membrane, and A is the active area of the membrane. The concentration of hydrogen at either face of the membrane is directly related to its pressure through Henry's law. Henry's constant (H) depends on the type of membrane and the gas in contact with the membrane.

$$C = HP \tag{8}$$

Combining Equations 7 and 8, we can express the diffusive flux as a function of cathode and anode pressures as:

$$\dot{n}_b = -DHA\frac{(P_c-P_a)}{d} \tag{9}$$

where DH is the permeability constant and depends on the nature of the gas and membrane. The procedure to obtain the value of DH will be presented shortly. Hydrogen can be assumed to follow the ideal gas law, giving:

$$\dot{n}_n = \dot{n}_f - \dot{n}_b = \frac{\dot{P}_c V_c}{RT} \tag{10}$$

where $\dot{n}_n$ is the net molar flow rate of hydrogen to the cathode (mol/s), $\dot{P}_c$ is the rate of cathode pressure rise (Pa/s), and V_c is the pressurized volume on cathode side (m^3).

As shown in Figure 4a, hydrogen flux across the membrane changes with time during the compression process. The forward flux (red curve, obtained from Equation 4) decreases rapidly with time at the start of operation and eventually reaches a plateau, the backward flux (blue curve, obtained from Equation 9) increases with time until it attains an equilibrium value, and the net flux (green curve) also decreases with time as shown. When equilibrium is attained, the net flux of hydrogen through the membrane drops to zero and that is also when the cathode pressure reaches its equilibrium value $(\dot{P}_c = 0)$ as predicted by Equation 10. The flux curves in Figure 4a are integrated in time to obtain the respective moles transferred in Figure 4b. Figure 4 pertains to the supplied voltage of 0.075 V; similar curves are observed for all the other voltages tested here.
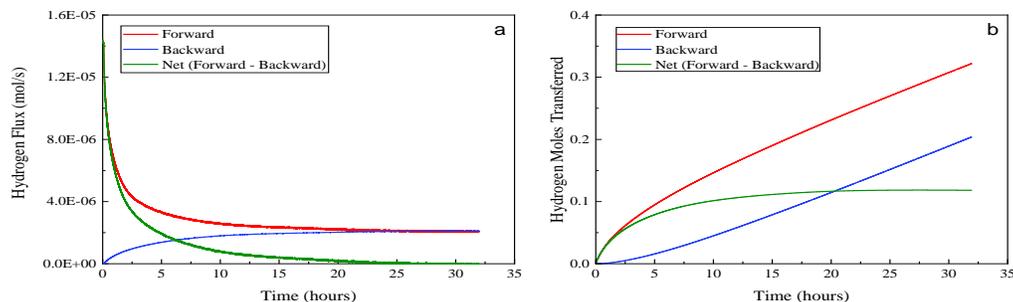
Figure 4. (a) Hydrogen flux through the membrane, and (b) moles transferred at 0.075 V.

Using Equations 4 and 9, Equation 10 can be rewritten to express both current and pressure as functions of time:

$$\frac{I(t)}{2F} - \frac{DHA\left(P_c(t) - P_a\right)}{d} = \frac{\dot{P}_c(t)V_c}{RT} \tag{11}$$

Equation 11 accounts for the role of back diffusion in the compression process by incorporating the backward flux term $(\dot{n}_b)$. It also provides insight about the electrochemical compression process in three distinct stages:

Initial Condition: At the start of the compression process $(t = 0)$, both anode and cathode are at atmospheric pressure, hence there is no back diffusion $(\dot{n}_b = 0)$. We can then rewrite Equation 11 as:

$$V_c = \frac{IRT}{2F\dot{P}_c} \tag{12}$$

Using the known values of I and $\dot{P}_c$ at $t = 0$ from Figure 2, we obtain the value of V_c as 23.87, 24.98, 24.28 and 23.49 cm³, respectively, for 0.025, 0.05, 0.075 and 0.10 V. The strong agreement between the V_c values across the different voltages is reassuring. The mean value of V_c is 24.15 cm³ which is a reasonable estimate for the cathode chamber volume.

Equilibrium: When the pressure reaches its equilibrium value, $\dot{P}_c = 0$. In an ideal scenario without back-diffusion, the equilibrium current would also reduce to zero. However, in reality, the forward flux equals the backward flux at steady state, and hence, there is an equilibrium current which maintains the cathode at equilibrium pressure $(P_{c,eq})$ given by:

$$I_{eq} = \frac{2FDHA\left(P_{c,eq} - P_a\right)}{d} \tag{13}$$

Using the measured equilibrium currents at the four applied voltages, Equation (13) can be rewritten to calculate the permeability constant:

$$DH = \frac{I_{eq}d}{2FA\left(P_{c,eq} - P_a\right)} \tag{14}$$

The average value of DH for the four voltages tested was $8.61E - 15 \text{ molPa}^{-1}\text{m}^{-1}\text{s}^{-1}$ which closely matches the values for Nafion 115 found in the literature [18-21].

Depressurization: When the equilibrium pressure is attained and the applied voltage is reset to zero ensuring there is no forward flux $(I = 0)$, the system is then allowed to depressurize. The hydrogen diffusing from the cathode to the anode can be detected by the formation of gas bubbles when the anode outlet tube is immersed in water. In this situation, the rate of cathode depressurization is determined solely by the backward flux and can be obtained by setting $I = 0$ in Equation 11:

$$\dot{P}_c = -\frac{DHART\left(P_c - P_a\right)}{dV_r} \tag{15}$$

Equation 15 can be integrated in time to show that the cathode pressure follows an exponential behavior while depressurizing:

$$P_c(t) = P_a + \left(P_{c,eq} - P_a\right)\exp\left(-\frac{DHART}{dV_r}t\right) \tag{16}$$

where $P_c(t)$ is the time-varying cathode pressure during depressurization, P_a is the (constant) anode pressure, and $P_{c,eq}$ is the equilibrium cathode pressure at the start of depressurization $(t = 0)$.

As shown in Figure 5, the cathode was depressurized after attaining an equilibrium pressure of 60 bara by setting the applied voltage to zero. The anode was continuously supplied with fully humidified hydrogen during depressurization to mirror the operating conditions during pressurization and ensure that the membrane does not dry out during depressurization thereby altering the value of $\mathcal{DH}$. Figure 5 shows that the measured rate of depressurization exactly matches the exponential curve fit from equation (16). From the curve fit, the value of the constant $\frac{\mathcal{DH}ART}{dV_c}$ is found to be $1.76E - 5\ s^{-1}$. Substituting the known values of A, R, T and d, we obtain the value of $\frac{\mathcal{DH}}{V_c}$ as $3.59E - 10\ molPa^{-1}m^{-4}s^{-1}$. Substituting $\mathcal{DH} = 8.61E - 15\ molPa^{-1}m^{-1}s^{-1}$ as found earlier, we obtain $V_c = 23.98\ cm^3$, which is consistent with the values obtained from Equation 12.
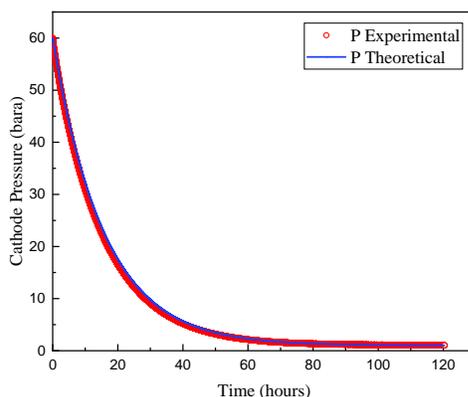

Figure 5. Pressure profile during cathode depressurization (experimental curve and exponential curve fit).

As stated earlier, a thicker membrane is better able to mechanically withstand the large pressure differentials obtained during ECC. At the same time, a thicker membrane would proportionally reduce back-diffusion. Therefore, there is a double benefit to increasing membrane thickness. However, a thicker membrane would increase ohmic losses, but this may be tolerable under the low voltage conditions employed during ECC. Future studies should be aimed at controlling back diffusion by either reducing the membrane's hydrogen permeability or increasing the membrane's thickness. The results obtained in this work also offer valuable insights into the effect of back-diffusion in the ECC efficiency [22] and stack design [23].

4. CONCLUSION

Electrochemical compression of hydrogen was demonstrated using a single-cell apparatus. It was possible to achieve pressures exceeding 150 bar with a small operating voltage of 0.1 V. This work focused on the role of back-diffusion in limiting the performance of an electrochemical hydrogen compressor. At higher pressures, the rate of back-diffusion increases, which in-turn creates a barrier in achieving even higher pressures. A theoretical formulation for the electrochemical compression process including back-diffusion was proposed and experimentally validated. The ability to achieve high pressures at modest voltages using an electrochemical hydrogen compressor makes it an attractive alternative to conventional mechanical compressors. However, back diffusion limits performance, therefore novel membranes with lower hydrogen diffusivities are highly desirable.

REFERENCES

1. DOE Technical Targets for Onboard Hydrogen Storage for Light-Duty Vehicles | Department of Energy [Internet]. Available from: https://www.energy.gov/eere/fuelcells/physical-hydrogen-storage.

2. S.H. Langer, R.G. Haldeman, "Electrolytic hydrogen purification and recovery of same," US Patent 3,475,302A (1969).

3. H.J.R. Maget, "Process for gas purification," US Patent 3,489,670A (1970).

4. B. Rohland, K. Eberle, R. Ströbel, J. Scholta, J. Garche, "Electrochemical Hydrogen Compressor," *Electrochimica Acta*, 1998, 43, 3841-3846.

5. R. Ströbel, M. Oszcipok, M. Fasil, B. Rohland, L. Jörissen, J. Garche, "The Compression of Hydrogen in an Electrochemical Cell Based on a PE Fuel Cell Design," *Journal of Power Sources*, 2002, 105, 208-215.

6. G. Sdanghi, G. Maranzana, A. Celzard, V. Fierro, "Review of the current technologies and performances of hydrogen compression for stationary and automotive applications," *Renewable and Sustainable Energy Reviews*, 2019, 102, 150–170.

7. J.M. Sedlak, J.F. Austin, A.B. LaConti, "Hydrogen recovery and purification using the solid polymer electrolyte electrolysis cell," *International Journal of Hydrogen Energy*, 1981, 6(1), 45–51.

8. T. Wong, F. Girard, T. Vanderhoek, "Electrochemical hydrogen compressor," US Patent US20040211679 (2004).

9. P.J. Bouwman, J. Konink, D. Semerel, L. Raymakers, M. Koeman, W. Dalhuijsen, E. Milacic, M. Mulder, "Electrochemical hydrogen compression," *Journal of the Electrochemical Soc*iety, 2014, 64(3), 1009–18.

10. P.J. Bouwman, "Advances In Electrochemical Hydrogen Compression And Purification," *Journal of the Electrochemical Soc*iety, 2016, 75 (14), 503-510.

11. M. Nordio , F. Rizzia , G. Manzolini , M. Mulder , L. Raymakers , M. V. S. Annaland , F. Gallucci, "Experimental and modelling study of an electrochemical hydrogen compressor," *Chemical Engineering Journal,* 2019, 369, 432-442.

12. M. Suermann, T. Kiupel, T. J. Schmidt, F. N. Buchi, "Electrochemical Hydrogen Compression: Efficient Pressurization Concept Derived from an Energetic Evaluation" *Journal of The Electrochemical Society*, 2017, 164 (12), F1187-F1195.

13. S.A. Grigoriev, I.G. Shtatniy, P. Millet, V.I. Porembsky, V.N. Fateev, "Description and characterization of an electrochemical hydrogen compressor/concentrator based on solid polymer electrolyte technology," *International Journal of Hydrogen Energy,* 2011, 36(6), 4148-4155.

14. M.T. Nguyen, S.A. Grigoriev, A.A. Kalinnikov, A.A. Filippov, P. Millet, V.N. Fateev, "Characterisation of a electrochemical hydrogen pump using electrochemical impedance spectroscopy," *Journal of Applied Electrochemistry*, 2011, 41, 1033–1042.

15. K.A. Perry, G.A. Eisman, B.C. Benicewicz, "Electrochemical hydrogen pumping using a high-temperature polybenzimidazole (PBI) membrane," *Journal of Power Sources*, 2008, 177(2), 478-484.

16. B. L. Kee, D. Curran, H. Zhu, R. J. Braun, S. C. DeCaluwe, R. J. Kee, S. Ricote, "Thermodynamic Insights for Electrochemical Hydrogen Compression with Proton-Conducting Membranes," *Membranes* 2019, 9(7), 77

17. Larminie, James (1 May 2003). Fuel Cell Systems Explained, Second Edition. SAE International. ISBN 978-0-7680-1259-0.

18. M. Schalenbach, T. Hoefner, P. Paciok, M. Carmo, W. Lueke, D. Stolten, "Gas Permeation through Nafion. Part 1: Measurements", *The Journal of Physical Chemistry C*, 2015, 119(45), 25145−25155.

19. T. Sakai, H. Takenaka, E. Torikai, "Gas diffusion in the dried and hydrated Nafions." *Journal of the Electrochemical Soc*iety, 1986, 133(1), 88–92.

20. J. Jiang, A. Kucernak, "Investigations of fuel cell reactions at the composite microelectrode| solid polymerelectrolyte interface. I. Hydrogen oxidation at the nanostructured Pt|Nafion® membrane interface." *Journal of Electroanalytical Chemistry*, 2004, 567(1), 123–137.

21. K. Broka, P. Ekdunge, "Oxygen and hydrogen permeation properties and water uptake of Nafion® 117 membrane and recast film for PEM fuel cell," *Journal of Applied Electrochem*istry, 1997, 27(2), 117–123.

22. A. Chouhan, B. Bahar, A. K. Prasad, "Effect of back-diffusion on the performance of an electrochemical hydrogen compressor," *International Journal of Hydrogen Energy,* 2020, 45(19), 10991-10999

23. A. Chouhan, U. R. Aryal, B. Bahar, A. K. Prasad, "Analysis of an electrochemical compressor stack," *International Journal of Hydrogen Energy,* 2020, 45(56), 31452-31465

ACKNOWLEDGEMENT